FIRE AND MATERIALS
Fire Mater. 2004; **28**:355–385 (DOI: 10.1002/fam.832)

Flammability of oil-based painted gypsum wallboard subjected to fire heat fluxes

Frederick W. Mowrer*,†

Department of Fire Protection Engineering, University of Maryland, College Park, MD 20742, U.S.A.

SUMMARY

The flammability of painted gypsum wallboard (GWB) exposed to fire heat fluxes is investigated. GWB samples coated with multiple layers of alkyd/oil-based paint are subjected to constant incident heat fluxes of 35, 50 and 75 kW/m^2 in the Cone Calorimeter for periods of 5, 10 and 15 min. A number of coats of alkyd/oil-based interior semi-gloss enamel paint, including 1, 2, 4, 6 and 8 coats, are applied over a single coat of oil-based primer to the exposed surface of 16 mm (5/8 in.) thick type X GWB. Unpainted type X GWB is also evaluated under the same exposure conditions. The potential for upward flame spread based on the Cone Calorimeter results is evaluated. The occurrence of paint 'blistering' is observed to have a significant effect on the time to ignition and consequently on the potential for upward flame spread. Further work is needed to evaluate the conditions under which 'blistering' will occur and its effects on the potential for surface flame spread on painted gypsum wallboard. Copyright © 2004 John Wiley & Sons, Ltd.

KEY WORDS: Cone Calorimeter; fire model; flame spread; gypsum wallboard; oil-based paint

1. INTRODUCTION

Painted gypsum wallboard (GWB) is one of the most widely used interior wall and ceiling finishes in the United States and perhaps throughout the world. Consisting of a core of gypsum (calcium sulfate dihydrate) sandwiched between two paper facers, GWB is available in a range of standard sizes and thicknesses. Because of its low cost, ease of installation and desirable finish characteristics, the use of GWB has largely replaced the use of traditional lath and plaster in both residential and commercial applications.

In many fire scenarios involving painted GWB finishes, the exposed painted surface and paper facer have been observed to burn out locally when subjected to fire heat fluxes. Fire investigators frequently use such damage patterns to draw conclusions regarding the development of a fire [1]. In other scenarios, the painted surface and paper facer have been observed to propagate a fire. The objective of this study is to evaluate the potential for flame spread on painted GWB and to determine the exposure conditions under which flame propagation is expected to occur. Cone

*Correspondence to: F. W. Mowrer, Department of Fire Protection Engineering, University of Maryland, College Park, MD 20742, U.S.A.
†E-mail: fmowrer@eng.umd.edu

Received 1 February 2001
Accepted 24 June 2003

calorimetry has been used in conjunction with a flame spread model developed by Quintiere and co-workers [2,3,4] to perform this evaluation.

In this project, GWB samples painted with 1 to 8 coats of alkyd/oil-based interior paint over 1 coat of oil-based primer are subjected, along with unpainted samples, to heat fluxes of 35, 50 and 75 kW/m^2 in the Cone Calorimeter for periods of 5, 10 and 15 min. Three replicate tests are conducted for each coating–heat flux–duration combination. Since all burning is essentially completed within the first 5 min of each test, for practical purposes there are 9 replicate tests for each coating–heat flux combination. The different test durations were used to evaluate the deyhdration of the GWB; results of the dehydration study are reported elsewhere [5].

2. BACKGROUND

The potential fire hazards associated with multiple layers of surface coatings have been recognized and addressed to some extent, particularly in the United Kingdom [6,7]. As far back as 1954, Pickard [6] reported on the potential effects, both positive and negative, that paints and other surface coatings can have on the ignition and flame spread of combustible surfaces. More recently, Murrell and Rawlins [7] addressed the fire hazard of surfaces coated with multiple layers of paint following a number of fires, including the King's Cross Underground fire in London and a number of stairway fires in New York tenements, where this factor was perceived to be significant. They conducted standard tests with samples coated with 14 layers of paint, using a variety of 'aged' and 'unaged' oil-based and water-based finishes. For these samples, they observed that flame spread was supported only for imposed heat fluxes over 15 kW/m^2. They noted that poor adhesion and 'blistering' affects performance. They concluded that all existing paint films should be perceived as potentially flammable and that the end-use hazards of existing paint films should be appropriately ascertained and addressed.

In a previous study by McGraw and Mowrer [8,9], GWB samples were painted with 2 to 8 coats of a latex-based interior paint plus one coat of a latex-based primer, then subjected to heat fluxes of 25, 50 or 75 kW/m^2 in the Cone Calorimeter for periods of 5, 10 or 15 min. Unpainted samples were similarly evaluated. Results of this previous study suggest that these painted surfaces are not likely to spread a fire under ambient temperature conditions at imposed heat fluxes of less than approximately 75 kW/m^2, regardless of the number of paint coats, but that they may spread a fire at this heat flux and higher. The behavior of GWB coated with various layers of oil-based paint is of interest to see how its performance compares with that of GWB coated with latex-based paint.

3. SAMPLE PREPARATION

The GWB samples were prepared by first cutting 162 specimens, each 100 mm square, from sheets of 15.9 mm (5/8 in.) thick type X GWB obtained at a local home improvement center. The samples were all weighed and the masses of the unpainted samples were recorded. 27 of the 162 samples were set aside to serve as the unpainted samples. After each stage of preparation and before weighing and testing, the samples were stored in a conditioned laboratory at a temperature of approximately 20°C and a relative humidity of approximately 50% until dry.

The remaining 135 samples were coated with a single layer of oil-based interior primer and a single layer of alkyd/oil semi-gloss enamel using a paint roller. These samples were allowed to dry to an equilibrium moisture content between and after each application, then they were weighed and their masses were recorded. Of these 135 samples, 27 were set aside to serve as the 1-coat samples. The remaining 108 samples were then coated with a second layer of oil-based interior paint using a paint roller. After drying, these samples were weighed and their masses were recorded, and 27 of these samples were set aside to serve as the 2-coat samples. The remaining 81 samples were coated with two more layers of paint, with 27 of these samples set aside to serve as the 4-coat samples. This process was repeated two more times to yield 6-coat and 8-coat samples.

The samples were divided into three sets, with nine samples for each coating category included in each set. Sample set designations and corresponding heat fluxes were assigned as:

- Set 1–35 kW/m^2 exposure
- Set 2–50 kW/m^2 exposure
- Set 3–75 kW/m^2 exposure

Of the nine samples in each coating category for each heat flux, three were tested for 5 min, three for 10 min and three for 15 min. Since all burning was effectively completed within the first 5 min for samples that ignited, for purposes of flammability evaluation there were 9 replicate tests conducted for each heat flux–coating combination. The different test durations were used to evaluate the dehydration of the gypsum wallboard samples [5]; they did not influence the flammability evaluation.

The mass of each GWB specimen before painting was determined and recorded. These weights are provided in Table I(a) for Set 1, in Table I(b) for Set 2 and in Table I(c) for Set 3. The average mass of the 162 unpainted samples was determined to be 110.2 g. The volume of a sample is calculated to be $1.59 \times 10^{-4}\,m^3$ based on specimen dimensions of 100 mm × 100 mm × 15.9 mm. From this average sample mass and calculated volume, the average bulk density of an unpainted sample is calculated to be $693\,kg/m^3$. According to the manufacturer of the GWB used for this testing [10], the area density of the paper on the front surface is approximately $220\,g/m^2$ (45 lbs/1000 sq. ft), while that on the back surface is approximately $205\,g/m^2$ (42 lbs/1000 sq. ft). Thus, the mass of the paper on the exposed surface of a 100 mm square test specimen is approximately 2.2 g and would constitute approximately 2 per cent of the mass of an unpainted sample.

The individual and average sample mass data are presented in Tables I(a) to I(c). From these data, the individual and average masses associated with the different layers of paint can be determined. The average paint mass associated with the different layers of paint are shown in Figures 1 to 3 for sample sets 1 to 3, respectively, while the average application rate (mass/area) per coating for the three sample sets are shown in Figure 4. As evident in Figure 4, there was some variability in the application rate for each coating as well as between sample sets. The variability based on the number of coatings can be explained, at least in part, by the decreasing absorptance of the surface as additional paint coats are added, although this does not explain the increase in paint mass per coating that occurs between the 3rd/4th and 5th/6th applications. This variability as well as the variability between sample sets can only be described in terms of random variability in the application rate since all the samples were coated at the same times by the same person using the same technique. On average, each coating of paint or primer added approximately 0.7 g of mass to a GWB sample, although this value ranged from approximately

Table I(a). Data for sample set 1–35 kW/m^2 exposure samples.

Set No. 1 35 kW/m^2		Pre-test sample mass (g)						Flammability parameters				
Test No.	Sample	Unpainted	Primer +1 coat	Primer +2 coats	Primer +4 coats	Primer +6 coats	Primer +8 coats	Ignition time, t_{ig} (s)	Peak HRR (kW/m^2)	Total HR (kJ/m^2)	Burning duration, t_0 (s)	Quintiere b factor
0003903	1	110.2						86.2	108.2	1804.6	16.7	−5.1
0003909	2	112.8						92.4	106.6	1539.4	14.4	−6.3
0003910	3	116.5						125.9	72.7	1328.4	18.3	−7.2
0003911	4	112.6						117.3	83.3	1502.2	18.0	−6.7
0003912	5	113.1						115.1	78.7	883.2	11.2	−10.5
0004502	6	109.1						104.6	90.4	1254.5	13.9	−7.6
0004508	7	107.6						87	91.6	1337.5	14.6	−6.0
0004514	8	110.8						89.3	99.8	1430.1	14.3	−6.2
0004804	9	113.7						113.1	69.7	1426.2	20.5	−5.8
0003904	10	109.0	110.6					67	48.3	756.1	15.7	−4.8
0003717	11	109.0	110.8					113.7	101.9	1070.8	10.6	−10.8
0004503	12	110.4	112.2					NI	NI	NI	NI	NI
0004509	13	106.6	108.1					88.8	90.4	1115.7	12.3	−7.3
0004515	14	106.5	107.9					102.7	57.9	1154.4	19.9	−5.6
0004805	15	111.3	112.6					92	51.9	1500.4	28.9	−3.7
0004810	16	109.3	110.6					76	50.3	1470.6	29.2	−3.1
0004815	17	112.6	114.0					120.1	33.2	631.5	19.0	−7.0
0005205	18	109.6	111.0					104.6	74.7	1202.2	16.1	−6.8
0003905	19	110.6	112.0	112.7				80.2	37.7	624.7	16.6	−5.5
0003916	20	108.1	109.6	110.3				69.7	64.1	1473.6	23.0	−3.4
0004504	21	110.3	112.1	112.5				98.9	108.2	1501.6	13.9	−7.0
0004510	22	108.9	110.7	111.3				76.6	85	1152.8	13.6	−5.8
0004516	23	108.5	110.1	110.6				76.1	100.1	1351.9	13.5	−5.6
0004806	24	110.7	112.4	113.0				NI	NI	NI	NI	NI
0004811	25	112.7	114.0	114.6				101.9	56.6	986.2	17.4	−6.3
0004816	26	111.9	113.1	113.8				72.3	74	1522.5	20.6	−3.8
0005206	27	111.0	112.3	113.0				NI	NI	NI	NI	NI
0003906	28	106.9	108.3	109.0	110.3			68	210	2015.8	9.6	−6.0
0003915	29	109.7	111.0	111.7	113.2			78	188.9	2068.1	10.9	−6.2

0004505	30	112.6	113.9	114.7	116.1			75	165.3	2368.7	14.3	−4.6
0004511	31	111.0	112.6	113.2	114.5			61.2	175.9	2435.1	13.8	−3.7
0004517	32	108.8	110.3	111.1	112.4			59.3	124.2	2599.3	20.9	−2.6
0004807	33	112.4	114.2	114.9	116.1			73.5	97.5	2525.5	25.9	−2.9
0004812	34	111.5	113.5	114.2	115.6			70	89	2368.6	26.6	−2.7
0004817	35	113.1	114.8	115.5	116.8			71.3	121.4	2328.5	19.2	−3.5
0005207	36	113.3	114.7	115.2	116.5			70.8	104.8	1857.6	17.7	−3.9
0003907	37	113.1	114.4	115.0	116.3	117.8		87.2	155.7	2627.9	16.9	−4.6
0003914	38	111.2	112.5	113.4	114.5	116.1		82	169.2	3514.5	20.8	−3.3
0004506	39	112.0	113.4	114.1	115.4	117.0		79	270	2992.2	11.1	−5.4
0004512	40	112.3	113.9	114.6	116.0	117.4		88.8	190.6	3082.3	16.2	−4.6
0004802	41	108.8	110.5	111.1	112.4	113.9		71.6	144.3	3198.2	22.2	−2.8
0004808	42	108.6	110.1	111.0	112.4	113.7		97.7	123	2700.7	22.0	−4.2
0004813	43	111.2	113.1	113.7	115.1	116.9		54.3	86.8	3072.4	35.4	−1.7
0004818	44	112.4	114.2	114.8	116.0	117.7		70.1	159	3207.3	20.2	−2.9
0005208	45	108.5	110.2	111.0	112.5	114.0		22.6	123.7	1954.1	15.8	−1.2
0003908	46	107.2	106.1	106.7	108.0	109.6	110.3	20.3	206.7	2672.4	12.9	−0.5
0003913	47	108.9	110.5	111.1	112.2	113.6	114.5	24.2	190.7	2406	12.6	−1.0
0004507	48	110.4	112.1	113.0	114.1	115.7	116.3	18	135.9	2377.2	17.5	−0.7
0004513	49	109.8	111.3	112.1	113.3	114.7	115.5	25.7	185.5	2776.8	15.0	−0.9
0004803	50	113.5	115.2	115.7	116.9	118.4	119.2	35	80.3	2757.2	34.3	−1.2
0004809	51	112.0	113.8	114.5	116.0	117.5	118.3	25	138.3	2943	21.3	−0.8
0004814	52	110.2	111.9	112.6	113.9	115.6	116.5	25.6	144.9	2965.2	20.5	−0.8
0004819	53	105.1	106.6	107.3	108.6	110.2	110.9	22.6	154.1	3641.7	23.6	−0.4
0005209	54	107.5	109.2	110.1	111.6	113.2	113.9	21.8	162.9	3160.2	19.4	−0.5
	Average	110.5	111.7	112.6	114.0	115.2	115.0					

Table I(b). Data for sample set 2–50 kW/m^2 exposure samples.

Set No. 2 50 kW/m^2		Pre-test sample mass (g)						Flammability parameters				
Test No.	Sample	Unpainted	Primer +1 coat	Primer +2 coats	Primer +4 coats	Primer +6 coats	Primer +8 coats	Ignition time, t_{ig} (s)	Peak HRR (kW/m^2)	Total HR (kJ/m^2)	Burning duration, t_0 (s)	Quintiere b factor
0000502	1	112.4						44	98	2078	21	−2.1
0000503	2	112.1						43	118	1736	15	−2.7
0000504	3	111.4						40	119	2316	19	−1.9
0000505	4	113.6						40	113	2578	23	−1.6
0000506	5	108.8						NI	NI	NI	NI	NI
0000507	6	114.0						37	125	2377	19	−1.7
0000508	7	115.6						45	114	2719	24	−1.8
0000509	8	114.3						43	118	1830	16	−2.6
0000510	9	112.9						39	133	2688	20	−1.6
0000511	10	110.6	112.0					36	112	1963	17	−1.9
0000512	11	105.8	107.2					31	123	2983	24	−1.0
0000513	12	110.8	112.5					44	158	2010	13	−2.9
0000514	13	111.3	112.7					41	99	1779	18	−2.3
0000515	14	108.5	109.9					NI	NI	NI	NI	NI
0002401	15	105.7	107.1					27	94	1948	21	−1.4
0002402	16	105.5	106.9					42	139	1499	11	−3.5
0002403	17	110.8	112.2					41	128	1885	15	−2.5
0002703	18	111.5	112.8					64	113	1331	12	−5.3
0002704	19	107.3	108.6	109.4				39	134	2698	20	−1.6
0002705	20	109.6	111.0	111.7				42	123	2239	18	−2.1
0002706	21	109.1	110.5	111.2				41	140	2414	17	−2.0
0002707	22	110.4	111.7	112.5				42	161	2927	18	−1.7
0002708	23	107.6	108.9	109.8				35	136	2327	17	−1.7
0002709	24	109.5	110.8	111.6				43	141	2384	17	−2.1
0002710	25	107.9	109.4	110.1				34	150	2432	16	−1.6
0002711	26	106.0	107.5	108.2				35	134	2599	19	−1.5
0002712	27	110.4	111.9	112.6				49	121	2206	18	−2.5
0002713	28	104.9	106.4	107.3	108.4			15	110	3376	31	−0.4
0002714	29	105.8	107.2	108.0	109.2			11	141	3313	23	0.0

0002715	30	108.8	110.2	111.2	112.4			11	147	3411	23	0.0
0002716	31	108.1	109.4	110.2	111.5			14	141	3821	27	−0.1
0002717	32	107.6	109.1	110.1	111.3			14	130	1216	9	−1.1
0003802	33	108.7	110.4	111.4	112.6			9	180	1502	8	−0.3
0003803	34	110.4	111.6	112.5	113.8			13	114	4201	37	−0.2
0003804	35	107.3	109.0	110.1	111.2			10	168	1697	10	−0.3
0003805	36	107.5	109.2	110.2	111.4			11	187	1713	9	−0.3
0003806	37	110.4	111.9	112.6	113.9	115.6		14	182	4898	27	0.3
0003807	38	109.9	109.5	110.3	111.5	113.2		10	225	2711	12	0.4
0003808	39	110.4	111.9	112.7	113.9	115.4		11	235	2557	11	0.3
0003809	40	108.9	110.4	111.1	112.3	113.9		10	224	2326	10	0.3
0003810	41	104.9	106.4	107.2	108.4	110.0		14	188	5056	27	0.3
0003811	42	107.9	109.1	109.9	111.0	112.8		15	259	4629	18	0.7
0003812	43	105.0	106.6	107.2	108.4	110.0		11	227	4677	21	0.7
0003813	44	115.3	116.9	117.5	118.8	120.9		14	222	2567	12	0.1
0003814	45	112.5	114.1	114.9	115.8	118.0		12	216	4152	19	0.6
0003815	46	109.5	111.1	111.7	113.0	114.6	115.5	11	233	5525	24	0.9
0003816	47	110.8	112.2	112.8	114.0	115.6	116.5	12	280	5435	19	1.2
0003817	48	109.8	111.4	111.8	113.1	114.9	115.7	12	242	5951	25	1.0
0003818	49	107.2	108.7	109.3	110.5	112.4	113.2	11	265	5587	21	1.1
0003819	50	112.2	113.6	114.1	115.3	117.1	117.8	13	248	2902	12	0.3
0003820	51	106.5	108.0	108.5	109.7	111.7	112.4	13	304	3454	11	0.9
0003821	52	109.3	110.8	111.2	112.3	114.1	114.8	12	241	4131	17	0.7
0003822	53	113.4	115.1	115.5	116.6	118.4	119.1	12	266	2943	11	0.6
0003823	54	109.8	111.4	111.8	112.7	114.4	115.0	12	225	3269	15	0.4
	Average	109.5	110.3	111.1	112.3	114.6	115.6					

Table I(c). Pre-test mass data for sample set 3–75 kW/m^2 exposure samples.

Set No. 3 75 kW/m^2		Pre-test sample mass (g)						Flammability parameters				
Test No.	Sample	Unpainted	Primer +1 coat	Primer +2 coats	Primer +4 coats	Primer +6 coats	Primer +8 coats	Ignition time, t_{ig} (s)	Peak HRR (kW/m^2)	Total HR (kJ/m^2)	Burning duration, t_0 (s)	Quintiere b factor
0005211	1	110.9						21	113	2389	21	−0.8
0005216	2	115.0						23	116	2170	19	−1.1
0005302	3	111.8						21	124	2171	18	−1.0
0005308	4	111.4						22	112	1970	18	−1.1
0005316	5	106.7						17	127	2355	19	−0.6
0005904	6	107.7						15	105	1708	16	−0.8
0005910	7	113.7						11	91	1512	17	−1.4
0006206	8	109.5						19	98	1870	19	−1.0
0006208	9	108.9						16	102	1762	17	−0.9
0005210	10	111.4	112.7					19	113	2809	25	−0.6
0005217	11	110.7	112.2					17	133	2599	20	−0.6
0005303	12	110.8	112.5					20	100	2510	25	−0.8
0005309	13	110.9	112.9					23	101	2255	22	−1.0
0005317	14	112.1	113.9					25	94	2297	24	−1.1
0005905	15	109.6	111.5					21	84	1887	23	−1.1
0005911	16	109.4	111.5					18	87	2200	25	−0.8
0006209	17	106.2	108.0					17	95	2193	23	−0.8
0006204	18	108.2	109.9					19	99	1980	20	−0.9
0005212	19	112.5	114.0	115.1				6	85	3150	37	−0.3
0005218	20	109.5	110.9	112.0				6	111	3237	29	−0.1
0005304	21	109.4	110.9	111.7				5	101	2890	29	−0.2
0005310	22	111.5	112.9	113.8				5	95	3406	36	−0.2
0005318	23	110.9	112.3	113.2				6	101	3302	33	−0.2
0005906	24	111.7	113.1	114.0				6	68	2402	36	−0.5
0005912	25	110.1	112.0	113.2				5	76	2692	35	−0.4
0006210	26	114.8	116.6	117.8				5	66	2705	41	−0.5
0006203	27	111.1	113.1	114.2				5	77	2738	36	−0.4
0005213	28	111.3	113.2	114.3	115.4			6	111	4669	42	0.0
0005219	29	108.0	109.9	110.7	111.8			5	155	4280	28	0.4

0005305	30	107.5	109.2	110.3	111.4		6	124	3798	31		0.1
0005311	31	110.8	112.5	113.4	114.6		5	138	4310	31		0.2
0005319	32	108.0	109.7	110.8	112.0		5	138	4080	30		0.2
0005907	33	107.7	109.4	110.6	111.7		5	102	3153	31		−0.1
0006202	34	110.2	112.0	113.0	114.4		5	99	3378	34		−0.2
0006211	35	111.0	112.6	113.9	115.2		6	93	3089	33		−0.2
0006207	36	112.3	114.0	115.0	116.2		5	91	3270	36		−0.2
0005214	37	113.0	114.8	115.9	117.0	119.0	6	187	6026	32		0.7
0005220	38	112.0	113.8	114.7	116.1	117.8	6	262	5391	21		1.3
0005306	39	105.4	107.3	108.1	109.7	111.3	6	235	5410	23		1.1
0005312	40	111.6	113.4	114.4	115.5	117.3	6	201	5368	27		0.8
0005314	41	111.0	112.8	113.6	115.1	116.7	6	192	4742	25		0.7
0005320	42	112.8	114.4	115.2	116.5	118.1	6	197	5037	26		0.7
0005908	43	112.6	114.3	115.2	116.6	118.4	6	151	4083	27		0.3
0006212	44	116.1	117.9	118.6	120.0	121.7	6	136	4306	32		0.2
0006205	45	109.9	111.7	112.5	113.7	115.4	7	136	4102	30		0.1
0005215	46	109.8	111.5	112.4	113.7	115.6	116.6	6	254	6516	26	1.3
0005221	47	107.5	109.2	110.0	111.1	113.0	113.9	6	335	5942	18	2.0
0005307	48	111.3	113.1	114.2	115.4	117.3	118.0	6	255	6034	24	1.3
0005313	49	115.7	117.3	118.4	119.6	121.2	121.9	6	251	4268	17	1.1
0005315	50	112.4	114.0	115.0	116.4	118.2	119.0	7	251	5799	23	1.2
0005903	51	113.8	115.5	116.7	117.9	119.9	120.8	6	231	4902	21	1.0
0005909	52	113.4	115.1	116.2	117.3	119.5	120.3	6	212	4757	22	0.9
0006213	53	110.0	111.7	112.7	114.0	116.1	117.0	7	212	5471	26	0.8
0006214	54	108.6	110.2	111.2	112.4	114.1	115.3	7	187	5094	27	0.6
	Average	110.7	112.5	113.7	114.8	117.3	118.1					

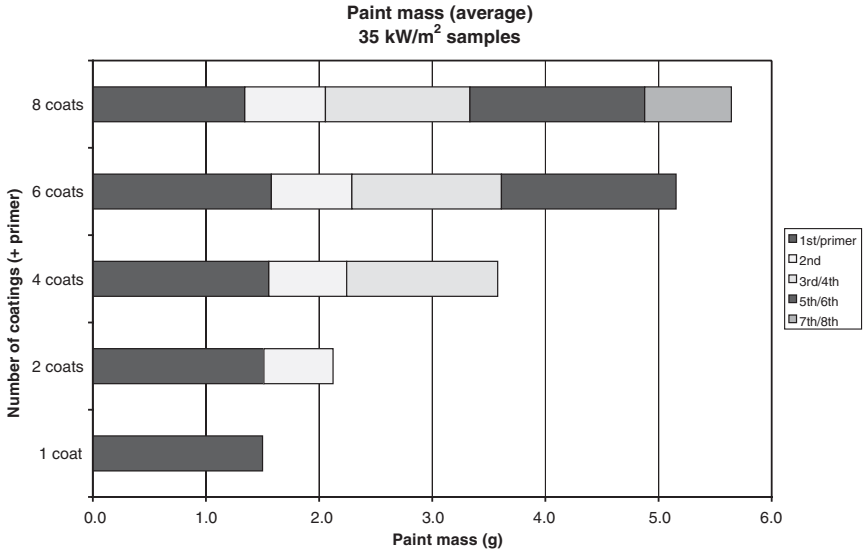

Figure 1. Average paint mass per sample for sample set 1–35 kW/m^2 heat flux.

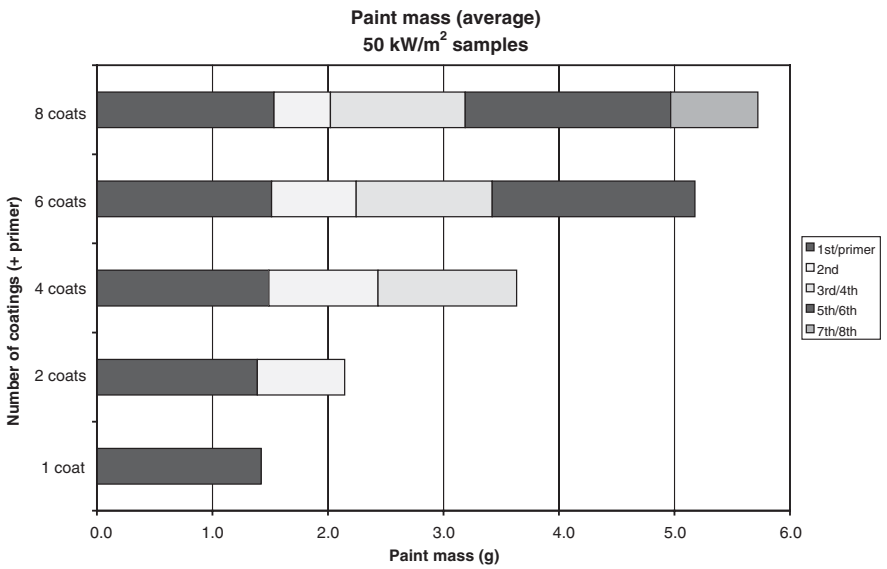

Figure 2. Average paint mass per sample for sample set 2–50 kW/m^2 heat flux.

0.4 to 1.0 g depending on the coating and set numbers. For the 0.1 m square GWB samples, this yields an application rate of 70 ± 30 g/m^2, as shown in Figure 4.

This application rate of 70 ± 30 g/m^2 was compared with product literature [11] on recommended application rates for the paint used in this project. In US units, a gallon (3.785 l) of the alkyd/oil semi-gloss enamel weighs approximately 11 pounds (5 kg) and has a

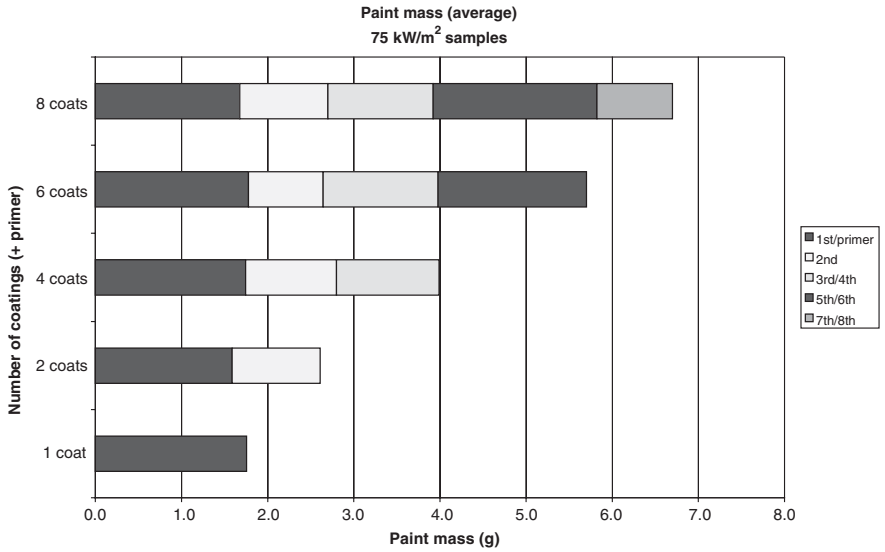

Figure 3. Average paint mass per sample for sample set 2–75 kW/m^2 heat flux.

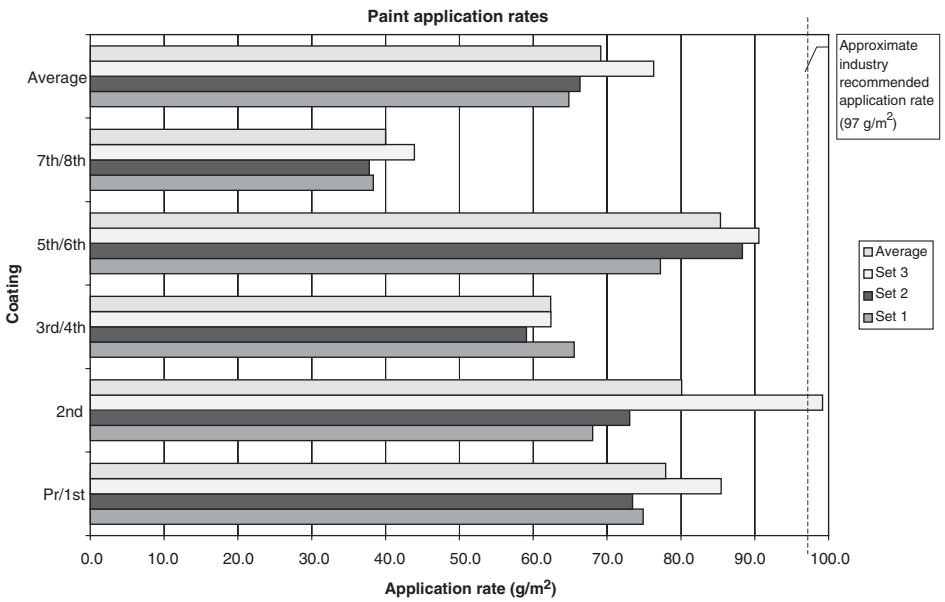

Figure 4. Paint application rates per coating (dry basis) for three sets.

recommended coverage of 400 square feet (37.2 m^2) per gallon on smooth surfaces, such as GWB. This yields a wet application rate of 134.5 g/m^2. The percent of solids by weight in this oil-based paint is approximately 72 per cent. Assuming this is the fraction of the weight remaining on the coated surface once the paint has dried, with the remaining fraction evaporated during the drying process, the recommended dry application rate would be

Table II. Reported composition of the alkyd/oil semi-gloss interior enamel used for this project.

Component	Percent of mixture
Calcium carbonate	6.2–25.2
Diatomaceous earth	0–2.6
Exempt mineral spirits	15.3–18.6
Hydrous aluminum silicate	0–16.1
Odorless mineral spirits	8.2–13.0
Oilseed compound	0–5.9
Synthetic resin complex	24.0–27.8
Titanium dioxide	0–21.6
Xylene	0.3–1.0
Zinc oxide	0–0.6

96.9 g/m^2. This would suggest that the average application rate during sample preparation was approximately 72 per cent of the recommended application rate for this paint.

The exact composition of the paint used for this project is not known; information provided in the material safety data sheet for this product [12] on the ranges for the various components on a wet basis is provided in Table II. Based on a review of these components, the only combustible component in this mixture after drying is believed to be the 'synthetic resin complex,' which constitutes approximately 25 per cent of the mixture weight on a wet basis and approximately 35 per cent of the mixture weight on a dry basis. The remaining 65 per cent of the paint coating on a dry basis would consist of the noncombustible components of the dried paint, including the calcium carbonate, diatomaceous earth, hydrous aluminum silicate, titanium oxide and zinc oxide identified in the material safety data sheet.

4. CONE CALORIMETER TESTS

Testing of the painted and unpainted GWB samples was performed in the Cone Calorimeter located in the Potomac Laboratory of the Department of Fire Protection Engineering at the University of Maryland. The Cone Calorimeter was calibrated and operated in general accordance with the procedures for Cone Calorimeter testing described in various standards [13, 14].

Heat release rates and mass loss rates were calculated in accordance with NFPA 271 [13] based on measured test data, including sample mass, exhaust mass flow rates and oxygen concentrations. Data were typically acquired every 2 s. The oxygen analyzer data was time-shifted to account for transport lag in the gas sampling line, but adjustments are not made for instrument response lags [15]. Data acquired during a test were imported into an Excel spreadsheet template, then heat release and mass loss calculations were performed in accordance with NFPA 271 within the spreadsheet template. These calculated parameters were then plotted on graphs within the template. Data and graphs for each test were then saved in Excel format under the filename associated with the test numbers shown in Tables I(a) to (c).

A heat release rate curve is shown in Figure 5(a) for a sample painted with four coats of paint plus primer that was exposed to a heat flux of 35 kW/m^2. Mass loss rate and total sample mass curves are shown in Figure 5(b) for the same sample. Similar curves are shown in Figures 6(a) and 6(b) for an imposed heat flux of 50 kW/m^2 and in Figures 7(a) and 7(b) for an imposed heat

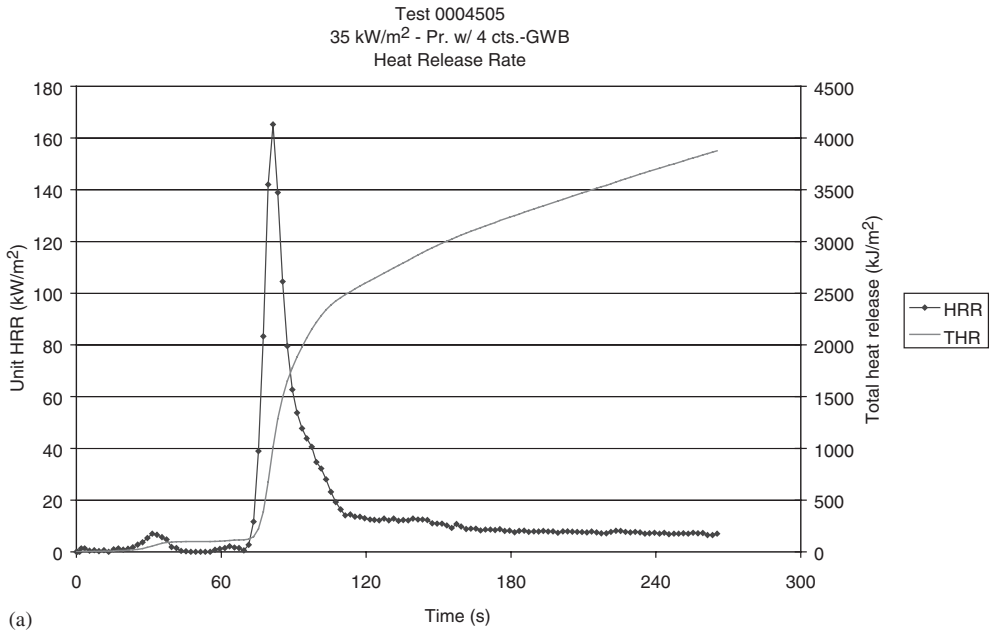

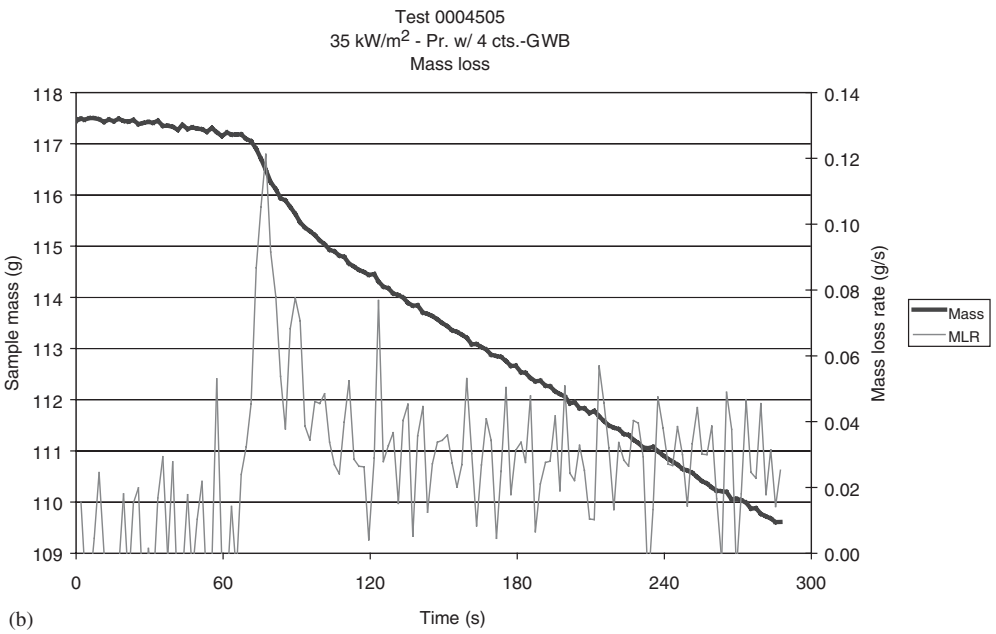

Figure 5. (a) Heat release rate and total heat release histories for Test 0004505–35 kW/m^2; and (b) mass loss rate and sample mass histories for Test 0004505–35 kW/m^2.

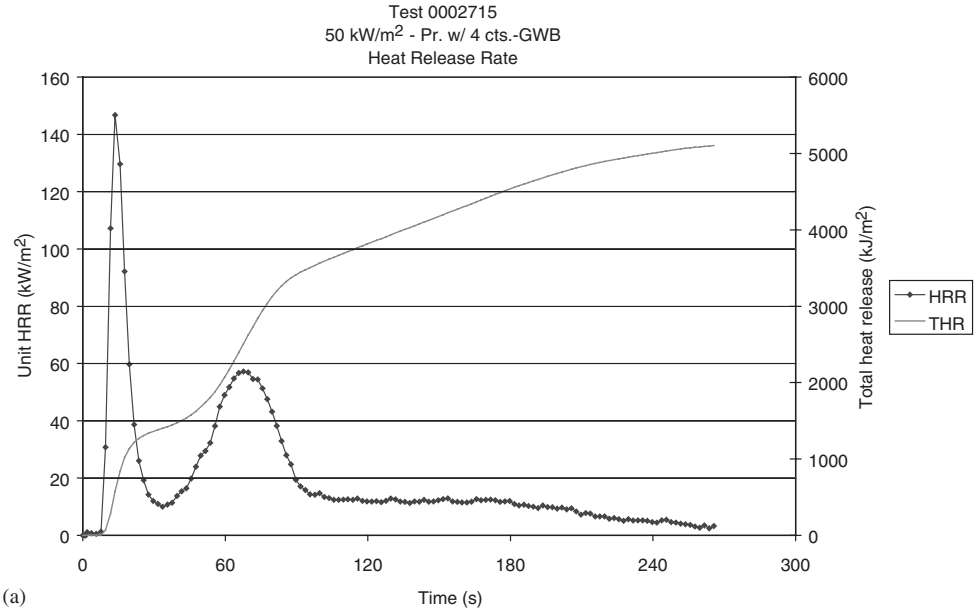

Figure 6. (a) Heat release rate and total heat release histories for Test 0002715–50 kW/m^2; and (b) mass loss rate and sample mass histories for Test 0002715–50 kW/m^2.

flux of 75 kW/m^2. Figure 8(a) shows heat release rate curves for samples with different coatings of paint subjected to an imposed heat flux of 35 kW/m^2. Figures 8(b) and 8(c) show similar data for imposed heat fluxes of 50 and 75 kW/m^2, respectively.

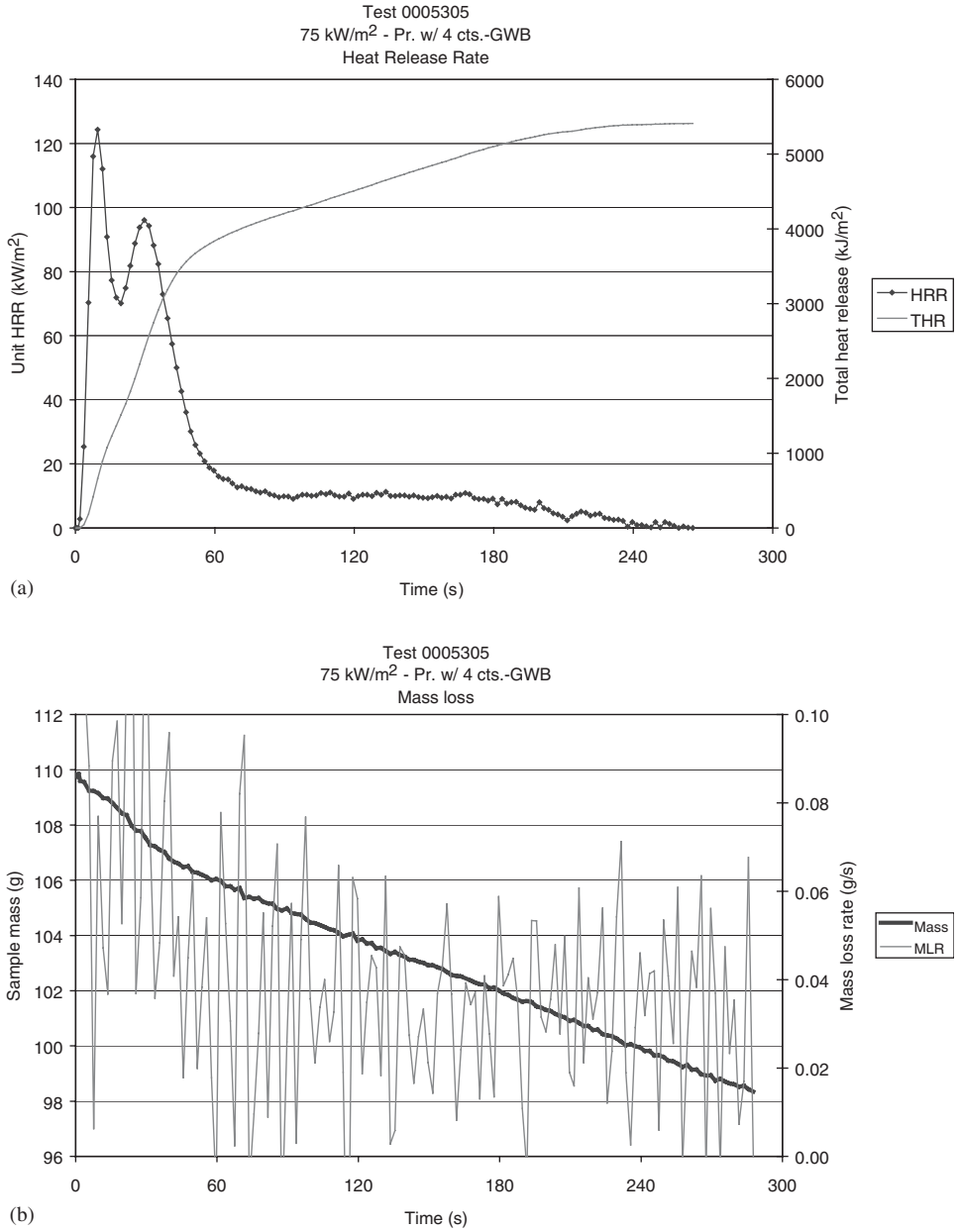

Figure 7. (a) Heat release rate and total heat release histories for Test 0005305–75 kW/m^2; and (b) mass loss rate and sample mass histories for Test 0005305–75 kW/m^2.

The ignition time of the GWB samples was measured in two ways. First, the data acquisition system for the Cone Calorimeter was used. In this procedure, a button on the Cone Calorimeter assembly is depressed when ignition is first observed and is held down as long as burning persists for up to 10 s. Based on this procedure, the Cone Calorimeter data acquisition program reports

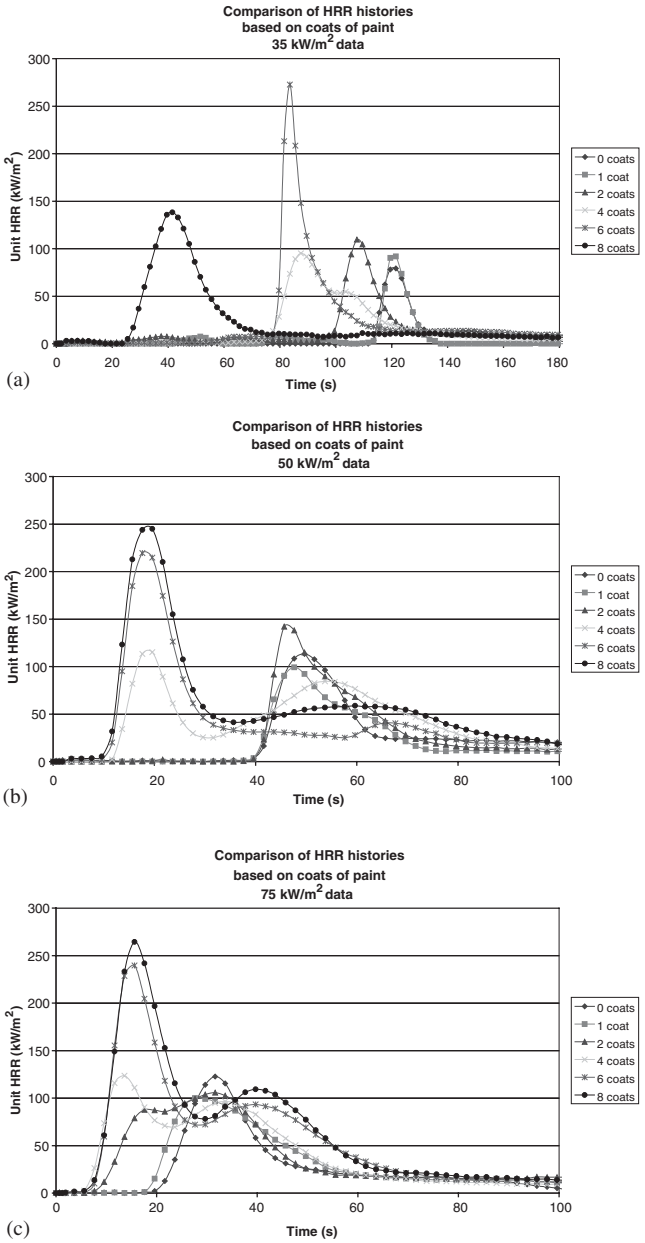

Figure 8. (a) Comparison of heat release rate curves for different coatings—35 kW/m^2; (b) comparison of heat release rate curves for different coatings—50 kW/m^2; and (c) comparison of heat release rate curves for different coatings—75 kW/m^2.

the time to ignition. Second, a stopwatch was used to measure ignition times manually, which were then recorded. While differences between the two methods are generally small, the second method consistently yielded more accurate ignition times, so these are the values that are

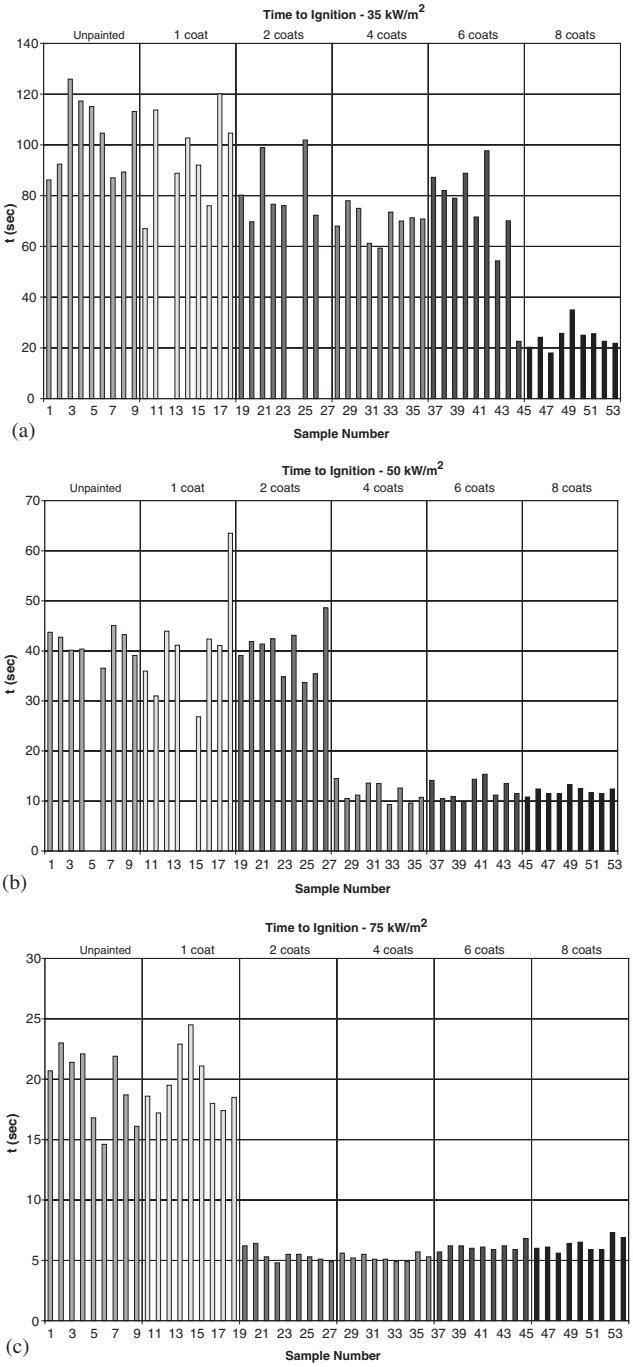

Figure 9. (a) Ignition times for data set 1–35 kW/m^2 heat flux; (b) ignition times for data set 2–50 kW/m^2 heat flux; and (c) ignition times for data set 3–75 kW/m^2 heat flux.

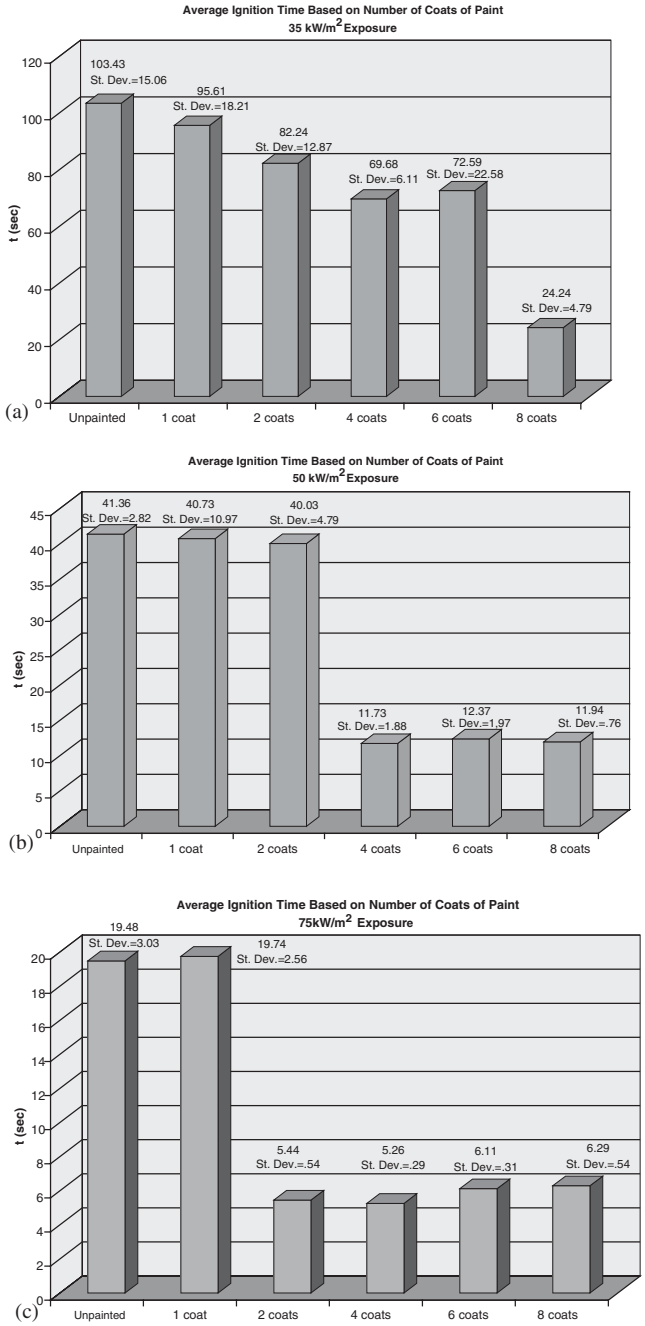

Figure 10. (a) Average ignition times for data set 1–35 kW/m^2 heat flux; (b) average ignition times for data set 2–50 kW/m^2 heat flux; and (c) average ignition times for data set 3–75 kW/m^2 heat flux.

reported. Differences between the two methods are most likely attributable to the finite scan rate of the data acquisition system as well as the reliance on human action for both methods.

The ignition times based on stopwatch data are shown in Tables I(a) to (c) for all samples. Ignition times are plotted for all samples in Figures 9(a) to 9(c) for data sets 1 to 3, respectively. Samples that did not ignite or for which data are not available are indicated by the absence of a time to ignition in the tables and figures. Average ignition times are plotted along with standard deviations in Figures 10(a) to 10(c) for data sets 1 to 3, respectively. Samples that did not ignite are not included in the average or standard deviation calculations.

An interesting phenomenon, 'blistering,' was observed during some of the Cone Calorimeter tests. When blistering occurred, the paint film would delaminate from the GWB substrate and form one or more bubbles above the GWB surface. Eventually, cracks would form in these bubbles, vapors would be ejected from these cracks under pressure, then ignition would occur. Blistering was accompanied by a marked decrease in the time to ignition, typically by a factor of 3 to 4 when compared with samples that did not blister. This is illustrated in Figures 9(a–c) and 10(a–c), which also show that the potential for blistering is a function of both the imposed heat flux and the number of coats of paint. At $35\,kW/m^2$, blistering was only observed for samples with eight coats of paint, except that one of the nine samples with six coats of paint also blistered. At $50\,kW/m^2$, blistering occurred for all samples with four or more coats of paint, but not for any samples with two coats of paint or less. At $75\,kW/m^2$, blistering occurred for all samples with two or more coats of paint, but not for any samples with one coat of paint or less.

When blistering of the surface occurred, it typically was initiated away from the edges, near the center of a sample. In some cases, a relatively large blister developed that covered almost the entire sample surface before bursting and deflating. In other cases, multiple smaller blisters would develop and burst. Reasons for these differences have not been determined. Under both circumstances, ignition tended to occur when the blisters burst and released vapors from within the blisters. The decrease in the time to ignition that was observed when blistering occurred may be due in part to the relative ease of heating the thin film of the blister and in part to the higher heat fluxes at the blister surface resulting from its closer proximity to the cone heater as it lifts from the surface.

5. ANALYSIS

The potential for upward or concurrent flow flame spread on painted GWB is evaluated based on the model developed by Quintiere and co-workers [2,3,4]. This model considers the potential for flame spread in terms of the ignition and burnout of surface elements as they are subjected to heat fluxes imposed by the flame and external sources. The details of the model and its simplifying assumptions are described elsewhere [2]. What is significant for the present discussion is that this flame spread model produces a dimensionless 'flammability parameter,' defined as:

$$b = k_f \dot{Q}'' - t_{ig}/t_b) - 1 \tag{1}$$

According to the Quintiere model, acceleratory upward flame spread is indicated when the value of the flammability parameter is positive, while decay to extinction is expected if its value is negative. Steady fire propagation is expected if the flammability parameter evaluates exactly as zero.

Evaluation of the flammability parameter requires evaluation of the respective parameters used to calculate it. Dillon *et al*. [16] discuss a number of ways to interpret Cone Calorimeter data for use with the Quintiere model. Mowrer and Williamson [17] describe a technique for using Cone Calorimeter data directly to evaluate these characteristic parameters and the associated flammability parameter for thin finish materials adhered to noncombustible substrates. These materials tend to exhibit distinct peaks in their heat release rate histories due to their relatively short burning durations. While originally developed for textile wallcoverings adhered to GWB, this technique should also be applicable to painted GWB, so it is used here. For a given incident heat flux, the ignition time (t_{ig}), the peak heat release rate per unit area ($\dot{Q}''$) and the total heat release per unit area (Q'') are measured and substituted directly into Equation (1). The ignition time in Equation (1) is the ignition time resulting from the heat flux associated with the wind-aided flame at the sample surface.

The peak heat release rate per unit area is calculated based on measurements made during a Cone Calorimeter test. Calculated values of the peak heat release rate per unit area are provided in Tables I(a) to (c) for all the specimens in the three data sets. They are also plotted in Figure 11 as a function of the number of coats of paint for each data set. It should be recognized that heat release rate curves with distinctive spikes have uncertainty in the peak value due to the finite data acquisition intervals, transport lags and instrument response characteristics [15]. Nonetheless, the calculated peak heat release rate per unit area is used here as representative of the actual performance.

The total heat release per unit area is the area under the heat release rate—time curve; the value used for analysis depends on the time frame of interest. As shown in Figures 5(a), 6(a) and 7(a), the total heat release per unit area is influenced by the heat release measured after the active burning period. The heat released during this period is not expected to contribute to the potential for flame spread, so it is ignored for present purposes and only the heat released during the active burning period is included in the calculation of the burning duration and hence the flammability parameter. For present purposes, this is somewhat arbitrarily defined as the time following the active burning period when the unit heat release rate first falls below $20\,kW/m^2$. This value is approximately coincident with the end of the active flaming period for these samples.

Calculated values of the total heat release per unit area are provided in Tables I(a) to (c) for all the specimens. They are also plotted in Figure 12 as a function of the number of coats of paint for each data set, where the primer coating is counted as one of the coats. Linear curve fits for each data set are also plotted in Figure 12. These curve fits can be used in conjunction with the surface paper basis weight and with the average paint application rate to deduce effective heats of combustion for the paper and the paint during the active burning period. These are shown in Table III for the three data sets.

The effective heats of combustion for both the paper and the paint demonstrate an increase with imposed heat flux, as shown in Table III. At the lower heat fluxes, more smoking of the sample occurs before ignition; this apparently contributes to lower combustion efficiency and consequently to a lower effective heat of combustion. The effective heats of combustion seem low, particularly for the paper, in comparison with published data. This is due, at least in part, to neglecting the heat released in the tail region of the heat release rate curves in the calculation of the effective heat of combustion during the active burning period. As illustrated in Figures 5(b), 6(c) and 7(c), only about 60 percent of the total heat release has been realized during the active burning period. If the effective heats of combustion shown in Table III are

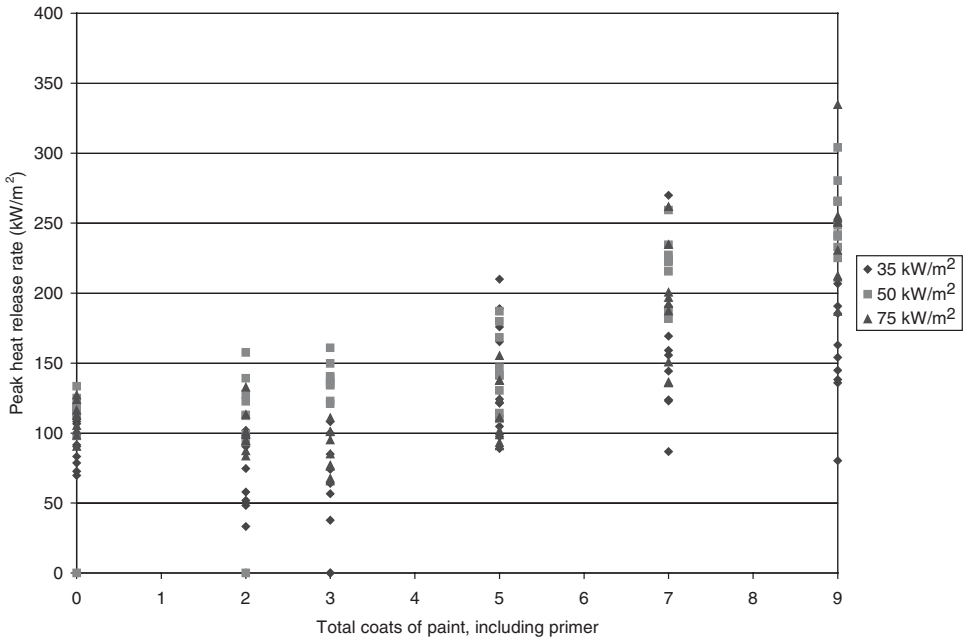

Figure 11. Peak heat release rate per unit area as a function of coats of paint for each data set.

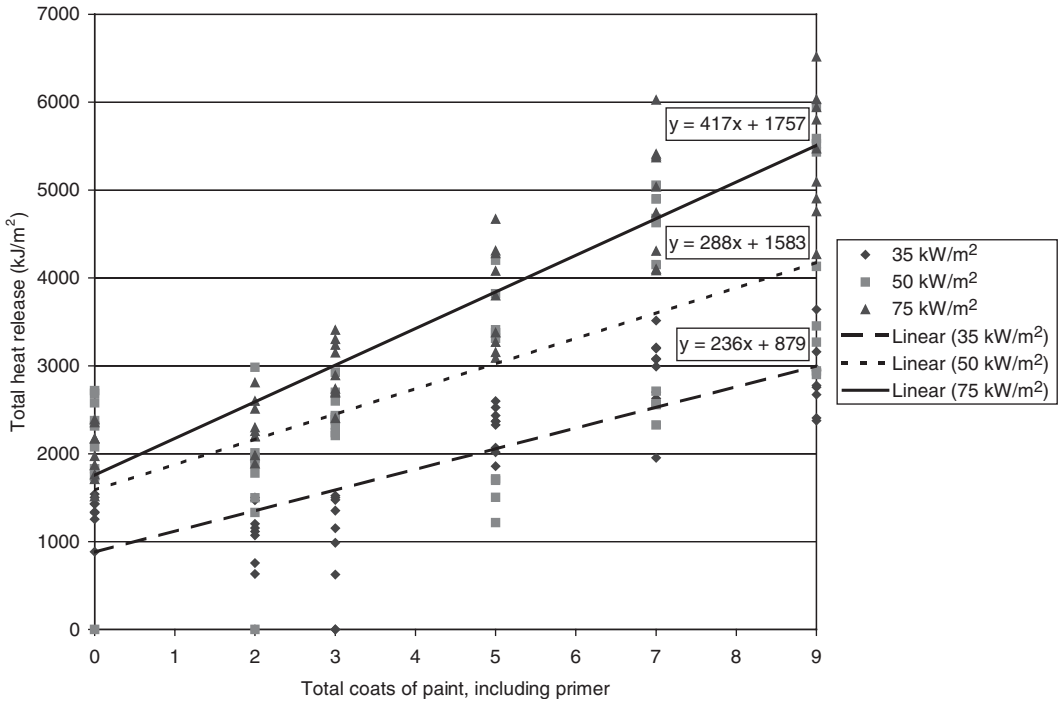

Figure 12. Total heat release per unit area as a function of coats of paint for each data set.

Table III. Effective heats of combustion for paper and paint.

Data set	Set 1	Set 2	Set 3
Imposed heat flux (kW/m^2)	35	50	75
Paper basis weight (g/m^2)	220	220	220
Heat release for paper only (kJ/m^2)	879	1583	1757
Paper effective heat of combustion (kJ/g)	4.0	7.2	8.0
Paint application rate (dry basis) (g/m^2/coating)	45.5	46.2	53.2
Paint heat release (kJ/m^2/coating)	236	288	417
Paint effective heat of combustion (dry basis) (kJ/g)	5.2	6.2	7.8
Paint effective heat of combustion (organic basis—35%) (kJ/g)	14.9	17.7	22.4

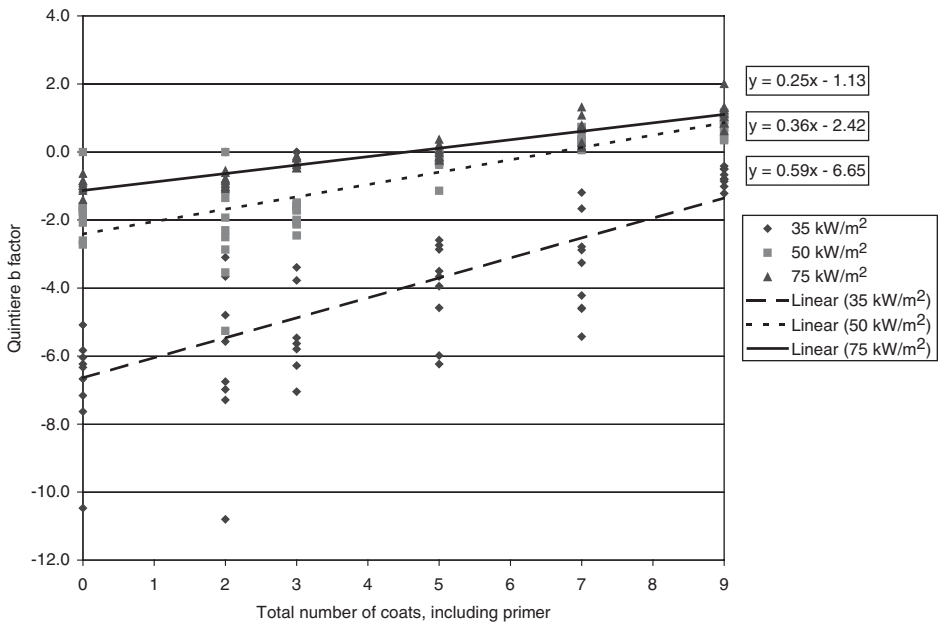

Figure 13. Calculated flammability parameter as a function of coats of paint for each data set.

normalized by a factor of 0.6 to account for this, values more consistent with literature values are achieved.

The flammability parameter expressed by Equation (1) was calculated for each specimen using the values for the ignition time, peak heat release rate per unit area and total heat release per unit area provided in Tables I(a) to (c). Calculated values of the flammability parameter for each specimen are shown in Tables I(a) to (c), where the flammability parameter is identified as the 'Quintiere *b* factor.' Calculated flammability parameters for each of the three data sets are plotted in Figure 13 as a function of the number of coats of paint. Linear curve fits are also plotted in Figure 13. In theory, the point where the flammability parameter becomes positive represents the point where acceleratory flame spread would be expected instead of local burnout. Based on the linear curve fits shown in Figure 13, this would occur at approximately 10 coats of paint (plus one coat of primer) at an imposed heat flux of $35\,kW/m^2$, between five and

six coats of paint (plus primer) at $50\,kW/m^2$ and between three and four coats of paint (plus primer) at $75\,kW/m^2$.

6. DISCUSSION

Whether a finish material will spread a flame or burn out locally can be considered as a race between the burning duration of an element that has been ignited and the time to ignition of an adjacent element being exposed to the heat flux from the burning element. If an element burns long enough to cause ignition of an adjacent element, flame spread can be expected; if not, then localized burnout would be expected. This is the essence of the Quintiere upward flame spread model.

The burning duration of an element is a function of the amount of fuel available in the element and the burning rate of the element. In turn, the burning rate of an element depends on the net heat flux at its surface. This can be expressed as:

$$t_b = \frac{Q''}{\dot{Q}''} = \frac{\rho\delta\Delta H_c}{\dot{q}''_{net}\left(\Delta H_c/L\right)} = \frac{\rho\delta L}{\dot{q}''_{net}} \tag{2}$$

where $\rho\delta$ is the combustible finish mass per unit area (kg/m^2), L is the effective heat of gasification (kJ/kg) of the finish material and $\dot{q}''_{net}$ is the net heat flux (kW/m^2) at the burning surface after ignition occurs. Equation (2) does not explicitly address combustion efficiency effects, which are assumed to be incorporated implicitly into the other terms.

The ignition time of an element depends on its thermophysical properties as well as on the imposed heat flux. Typically, finish materials are considered as either thermally thick or as thermally thin, depending on the thickness of the finish/substrate assembly as well as on the thermal properties of the assembly. For thermally thick materials subjected to a constant net heat flux at the surface, the ignition time can be expressed as:

$$t_{ig} = \frac{\pi}{4}\, k\rho c \left[\frac{\Delta T_{ig}}{\dot{q}''_{net}}\right]^2 \tag{3}$$

For thermally thin materials subjected to a constant net heat flux at the surface, the ignition time can be expressed as:

$$t_{ig} = \rho c\delta \left[\frac{\Delta T_{ig}}{\dot{q}''_{net}}\right] \tag{4}$$

In general, the net heat flux terms in Equations (2), (3) and (4) will not be equal to each other or constant. Nonetheless, the potential for flame spread can be evaluated, at least semi-quantitatively, by assuming the net heat fluxes in Equations (2), (3) and (4) are proportional to each other. With this assumption, the ratio between the burning duration, t_b, and the ignition time, t_{ig}, can be evaluated in terms of Equations (2), (3) and (4). If this ratio has a value greater than 1 (i.e., $t_b/t_{ig} > 1$), then a material would be expected to burn long enough for the adjacent element to ignite, in which case flame spread would be expected. For a thermally thick material, the ratio between the burning duration and the ignition time evaluates as:

$$\frac{t_b}{t_{ig}} = \chi_b \left(\frac{\rho\delta L}{IRP}\right) \dot{q}''_{net} \tag{5}$$

where the IRP is an ignition response parameter that is similar to the square of the thermal response parameter defined by Tewarson [18] for thermally thick materials and χ_b is an appropriate proportionality constant to account for the ratio between the different net heat fluxes in Equations (2) and (3) (i.e., $\dot{q}''_{net,Eq.2} = \chi_b \dot{q}''_{net,Eq.3}$) Consequently, for a thermally thick finish, flame spread would be indicated when

$$\dot{q}''_{net} > \chi_b \left(\frac{IRP}{\rho \delta L} \right) \tag{6}$$

This analysis suggests that there is a critical net heat flux for flame propagation on a thermally thick finish. At net heat fluxes above this critical threshold, upward flame spread would be expected, while localized burnout would be expected at lower heat fluxes. Equation (6) also shows that the critical net heat flux for flame propagation is expected to vary inversely with the coating application rate, which should be nominally proportional to the number of coatings. This is illustrated in Figure 14, which shows the number of coats of paint required to yield a positive flammability parameter as a function of the imposed heat flux based on the curve fits developed in Figure 13. A curve fit for the inverse relationship expected between the critical net heat flux for flame propagation and the number of coatings is also shown in Figure 14. The value of 356.5 used as the proportionality factor in this curve fit was determined as the average value of the heat flux–coating product for the three data points illustrated.

The effect of preheating can also be considered, at least qualitatively, in terms of Equation (6). Preheating of a surface would tend to decrease the effective value of the IRP by decreasing the surface temperature increase needed for ignition; it would also tend to decrease conduction losses into the surface. This would have the consequence of decreasing the value of the critical net heat flux for flame propagation. In the limit, as the surface temperature approaches the

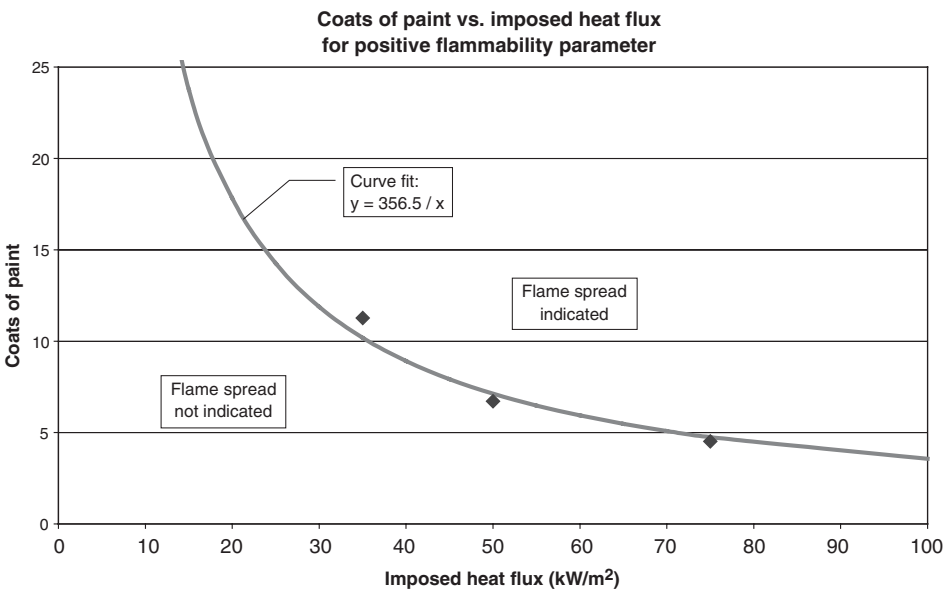

Figure 14. Number of coats of paint required to yield a positive flammability parameter.

ignition temperature, the critical net heat flux for flame propagation would decrease towards zero.

Attention is now returned to the painted GWB. While the previous discussion addresses some of the theoretical considerations related to the potential for flame spread, actual ignition times and burning durations were measured in the Cone Calorimeter tests. These measurements can be used directly to compare burning durations with ignition times at an imposed heat flux. In doing so, however, it should be recognized that the heat flux at the surface changes once the specimen ignites. Before ignition, the incident heat flux at the surface is simply that imposed externally by the Cone heater. Following ignition, this external heat flux is augmented by additional heat flux from the flame of the burning material. Some potential impacts of this are discussed below. But first, the burning durations and ignition times at a given imposed heat flux are discussed.

The ratio between the burning duration and the ignition time at a given heat flux is shown in Figure 15 for each data set. Figure 15 shows that, with one exception, the burning duration is always shorter than the ignition time for the $35\,kW/m^2$ data. For these data, the ratio between the burning duration and the ignition time is near unity only for the samples with eight coats of paint. These are the only samples that demonstrated blistering at this heat flux. Similarly, for the $50\,kW/m^2$ data, the burning duration is less than the ignition time for samples with two coats of paint or less and generally greater for samples with four coats of paint or more. This distinction is consistent with the occurrence of blistering at this heat flux.

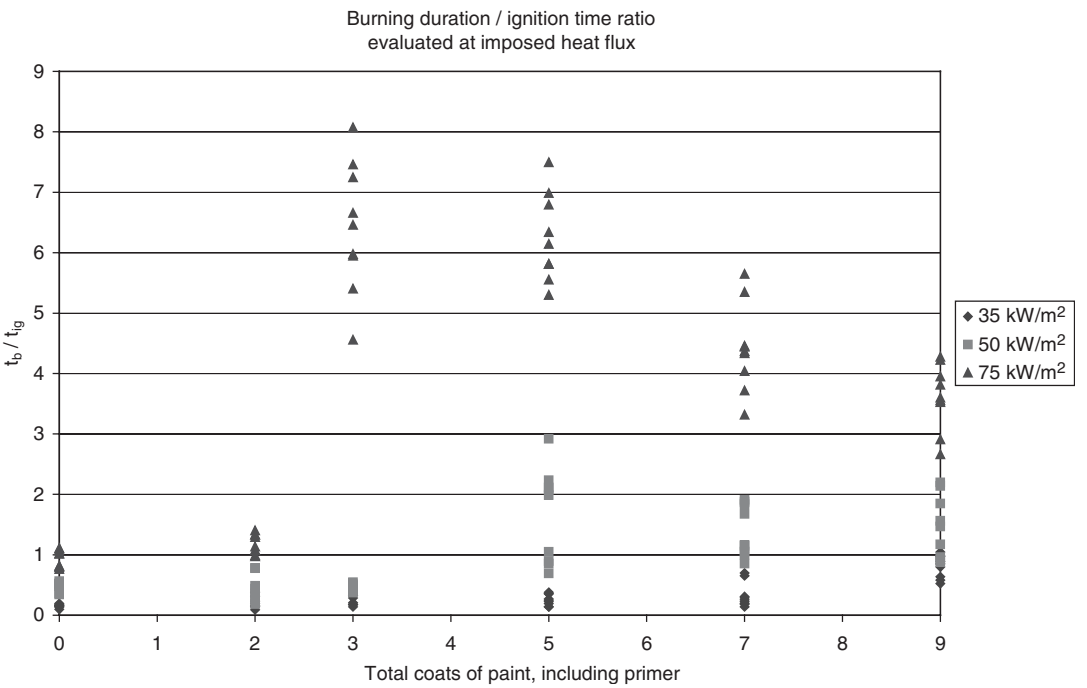

Figure 15. Burning duration to ignition time ratio as a function of coats of paint for each data set.

The distinction in the burning duration to ignition time ratio is even more pronounced for the 75 kW/m^2 data. For these data, samples with one coat of paint or less have burning duration to ignition time ratios near unity, while samples with two or more coats of paint have burning duration to ignition time ratios considerably greater than unity, ranging from 2.7 to 8.1. This performance is consistent with the occurrence of blistering at this heat flux and can be attributed at least in part to the 3- to 4-fold decrease in ignition times that accompanies blistering, as shown in Figures 9(a)–(c).

Specimens that do not blister are expected to behave as thermally thick materials. For thermally thick materials, the ignition response parameter is expected to remain constant. By assuming that the net heat flux is proportional to the imposed heat flux and that the proportionality constant, χ_{hf}, is independent of the magnitude of the heat flux, Equation (3) can be solved for an effective ignition response parameter in terms of the ignition time and the imposed heat flux as:

$$IRP_{\text{eff}} = \frac{IRP}{\chi_{\text{hf}}^2} \equiv \frac{\pi}{4} k\rho c \left[\frac{\Delta T_{\text{ig}}}{\chi_{\text{hf}}}\right]^2 = t_{\text{ig}} \left(\dot{q}''_{\text{ext}}\right)^2 = \text{const.} \tag{7}$$

The proportionality constant accounts for the fact that only a fraction of the imposed heat flux is absorbed at the surface, with the remaining fraction reradiated and convected from the surface.

The effective ignition response parameter expressed by Equation (7) is plotted as a function of the coats of paint in Figure 16 for all the specimens. Figure 16 clearly shows a difference in the

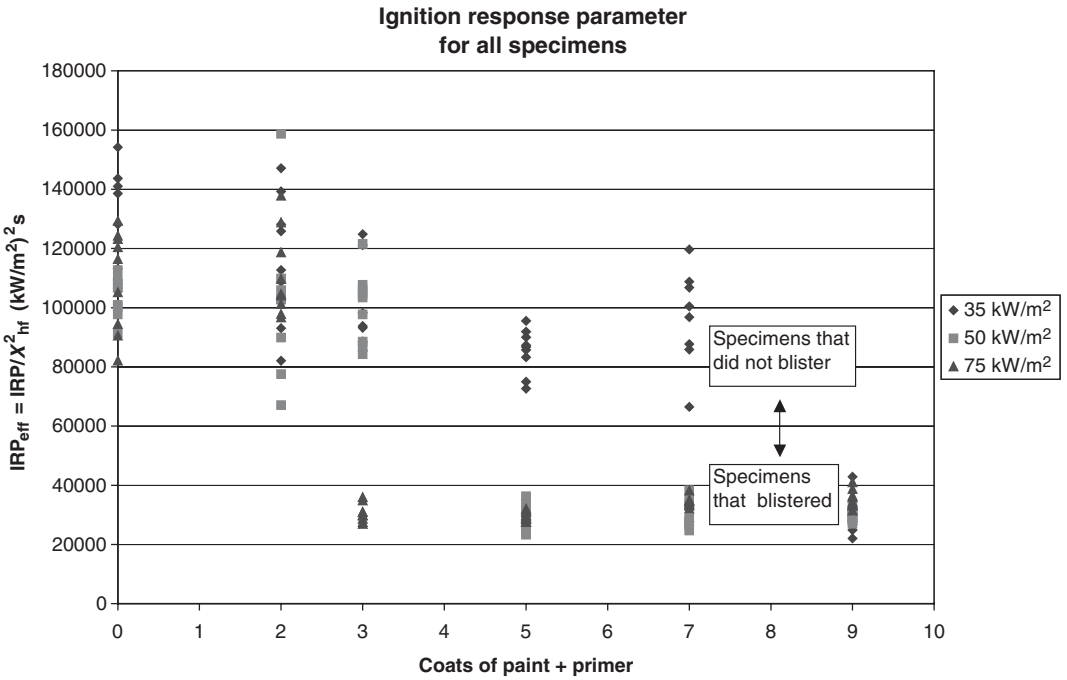

Figure 16. Effective ignition response parameter for all specimens.

effective ignition response parameter between specimens that blistered and those that did not. For the specimens that did not blister, the average value for the effective ignition response parameter was 105,374 $(kW/m^2)^2$-s, with a range of 66,518 to 158,750 $(kW/m^2)^2$-s. This compares with values of 104,977 $(kW/m^2)^2$-s for 'common' GWB and 75,430 $(kW/m^2)^2$-s for "FR" GWB based on thermal properties reported by Quintiere [19] that are derived from LIFT tests [20]. For specimens that did blister, the average effective ignition response parameter was 31,065 $(kW/m^2)^2$-s, with a range of 22,050 to 42,875 $(kW/m^2)^2$-s. On average, this represents a decrease by a factor of 3.4 in comparison with the specimens that did not blister.

The occurrence of blistering might reasonably be expected to change the flammability performance of a surface from that of a thermally thick material to that of a thermally thin material. For a thermally thin material, Equation (4) suggests that the total energy required for ignition should remain constant provided the ignition temperature is constant. By again assuming that the net heat flux is proportional to the imposed heat flux and that the proportionality constant, χ_{hf}, is independent of the magnitude of the heat flux, Equation (4) is rearranged to solve for what is termed here the effective specific ignition energy (SIE_{eff}):

$$SIE_{eff} \equiv \frac{c\Delta T_{ig}}{\chi_{hf}} = \frac{t_{ig}\dot{q}''_{ext}}{\rho\delta} \tag{8}$$

The effective specific ignition energy is plotted as a function of the total mass of paint and primer in Figure 17 for the specimens that blistered. From Figure 17, it is evident that the effective specific ignition energy is not quite constant as might be expected for a thermally thin material; it decreases with increasing coats of paint as well as with increasing heat flux. It is

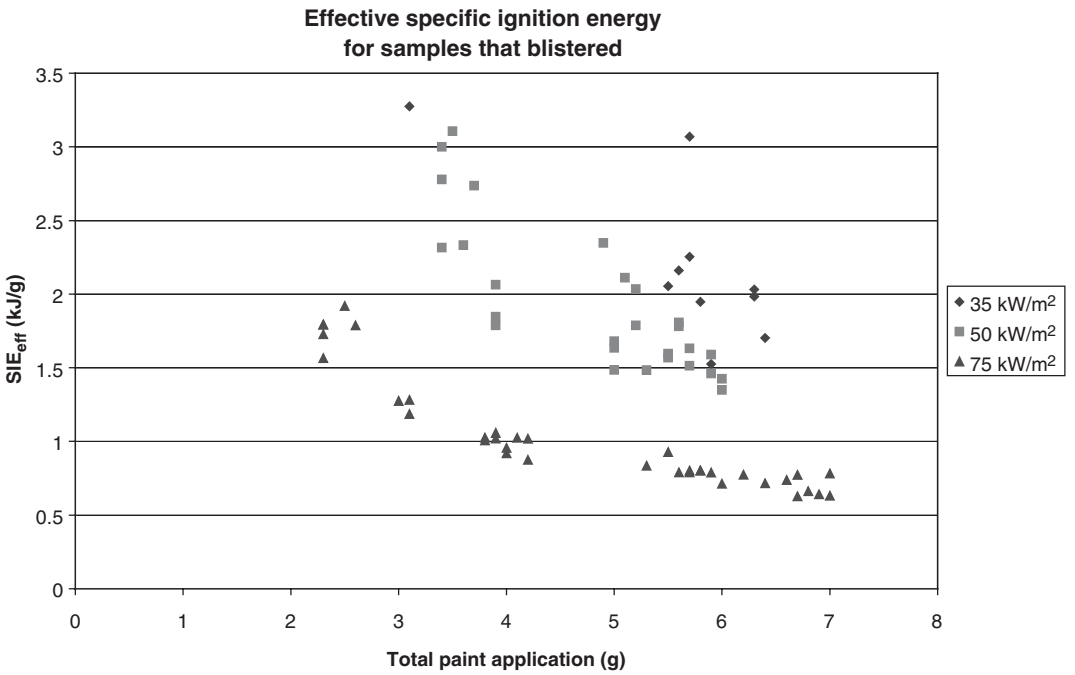

Figure 17. Effective specific ignition energy for specimens that blistered.

suspected that this behavior may be related to the permeability of the paint film, but the changing heat flux as the paint film expands towards the cone heater might also play a role.

Regarding the potential role that permeability might play, the following explanation is offered. As additional coats of paint are added, the permeability of the surface is expected to decrease. As moisture within the GWB evaporates and tries to escape from the surface, it is trapped by the paint film, causing a pressure increase that leads to blistering. As the imposed heat flux increases, the rate of moisture evaporation will increase, causing a larger pressure rise, and consequently blistering, earlier. The results in Figure 17 are consistent with these observations, but more work is needed to explore the effects of moisture evaporation and paint film permeability on the potential for blistering. The actual performance of painted surfaces that blister most likely falls somewhere between that expected of a thermally thick and a thermally thin material.

At this point, attention is returned to consideration of the effects of the flame heat flux. Quintiere and co-workers [21,22] investigated the magnitude of the flame heat flux in the Cone Calorimeter for a gas burner and for a range of thermoplastic materials burning under steady conditions. They concluded that the flame heat flux in the Cone Calorimeter is fairly constant for a given material provided the flame length is at least twice its effective diameter. They determined values of the flame heat flux that ranged from $14\,kW/m^2$ for polypropylene to $37\,kW/m^2$ for PMMA, with nylon and polyethylene having intermediate values of 30 and $25\,kW/m^2$, respectively.

Flame heat fluxes were not measured in the Cone Calorimeter tests reported here. The method described by Hopkins and Quintiere [21] for determining flame heat fluxes in the Cone Calorimeter only works for the quasi-steady burning conditions they described, not for the highly transient burning conditions observed here. Consequently, the effect of the flame heat flux in the Cone Calorimeter tests reported here is only addressed qualitatively.

Before a material ignites in the Cone Calorimeter, it is subjected only to the external heat flux imposed by the Cone heater. Consequently, the ignition time is that associated with the imposed heat flux. Once a material ignites in the Cone Calorimeter, it is subjected to the combination of the external heat flux and the flame heat flux. Consequently, the burning rate and the burning duration should be that associated with this combined, but unknown, heat flux. Therefore, it could be argued that the burning duration associated with the combined heat flux should be compared with the ignition time associated with the imposed heat flux only to evaluate the potential for flame spread at an imposed heat flux. On the other hand, the combined, but unknown, heat flux might be more similar to field conditions, where a fuel element will be subjected to an external heat flux until it ignites, then will be subjected to this external heat flux in addition to the heat flux from its own flame after it ignites. If this flame heat flux in the field is comparable to the flame heat flux in the Cone Calorimeter, then it would be reasonable to use the burning duration associated with the imposed heat flux to evaluate the potential for flame spread at that imposed heat flux. For the present analysis, this has been done.

7. SUMMARY AND CONCLUSIONS

The flammability characteristics of type X gypsum wallboard coated with different layers of an alkyd/oil interior paint have been evaluated. The same paint was used for all layers except the primer coat, which was also an oil-based paint. The Cone Calorimeter was used to evaluate

ignition and flammability characteristics under constant imposed heat fluxes of 35, 50 and 75 kW/m^2. Data derived from these Cone Calorimeter tests were used in conjunction with Quintiere's upward flame spread model to evaluate the potential for concurrent flow fire propagation on painted GWB surfaces.

This work suggests that there is a relationship between the number of coats of paint on a surface and the potential for upward flame spread. As the number of coats of paint increases, the critical heat flux to the surface required for flame propagation decreases. Below the critical heat flux for flame propagation, local burnout is expected, while above this critical heat flux, flame propagation might be expected. Large-scale fire tests would be useful to verify this conclusion under realistic enclosure fire conditions.

During the Cone Calorimeter tests, the phenomenon of blistering was observed where the film of paint would delaminate from the GWB substrate under the imposed heat flux. Blistering did not occur for all painted samples. Rather, the likelihood of blistering appeared to be a function of both the imposed heat flux and number of coats of paint, with more coats of paint being required at lower heat fluxes. When blistering did occur, the time to ignition decreased dramatically, typically by a factor of 3 to 4 when compared with samples where blistering did not occur. Since the potential for flame spread can be viewed as a race between the burnout of already ignited surfaces and the ignition of adjacent surface elements, such a reduction in the time to ignition would tend to tip the balance in favor of flame spread.

Further work is needed to explore the phenomenon of blistering and its effect on the potential for flame spread on painted or coated surfaces. This work should include substrates other than GWB, coatings other than the alkyd/oil-based paint considered here as well as the effects of aging and different combinations of paint/coating types on the potential for blistering. Blistering is an issue that affects the everyday performance of coatings and coated surfaces. Work related to this phenomenon under normal use conditions should be investigated to see if it can be applied to the prediction of blistering under fire conditions.

NOMENCLATURE

b	Quintiere flammability parameter (defined in Equation (1))
c	Specific heat (kJ/kg.K)
IRP	Ignition response parameter (kW/m^2)^2-s ($\equiv \pi 4k\rho c\Delta T_{ig}^2$)
k	Thermal conductivity (kW/m.K)
k_f	Characteristic flame length coefficient ($\sim$0.01 m^2/kW)
L	Fuel heat of vaporization (kJ/kg)
m''	Fuel mass per unit area of surface (kg/m^2) ($\equiv \rho\delta$)
Q''	Characteristic heat release per unit area (kJ/m^2)
$\dot{Q}''$	Characteristic heat release rate per unit area (kW/m^2)
$\dot{q}''_{net}$	Net heat flux to fuel surface (kW/m^2)
t_{ig}	Characteristic ignition time (s)
t_b	Characteristic burning duration (s) [$\equiv Q''/\dot{Q}''$]
T_{ig}	Effective ignition temperature (°C)
T_0	Ambient temperature (°C)
χ_b	Proportionality constant for net heat fluxes for ignition and for burning (−)
χ_{hf}	Fraction of imposed heat flux absorbed at fuel surface (−)

χ_{ig} Fraction of fuel that must be vaporized to form ignitable mixture at fuel surface (–)
δ Fuel surface thickness (m)
ΔH_c Fuel heat of combustion (kJ/kg)
ΔH_v Fuel heat of vaporization (kJ/kg)
ΔT_{ig} Ignition temperature rise above ambient ($T_{ig}-T_0$)
ρ Density (kg/m^3)

ACKNOWLEDGEMENTS

This work was supported by the Building and Fire Research Laboratory at the National Institute of Standards and Technology under the technical supervision of Mr. Daniel Madrzykowski. Sample preparation, Cone Calorimeter testing and data reduction and analysis were performed by Ms. Jamie Ferrino and Mr. Pedro Rodriguez while they were undergraduate students in the Department of Fire Protection Engineering at the University of Maryland. This financial support and testing assistance are gratefully acknowledged.

REFERENCES

1. Guide for Fire and Explosion Investigations. *NFPA 921*, National Fire Protection Association, 1998.
2. Saito K, Quintiere JG, Williams FA. Upward turbulent flame spread. *Fire Safety Science—Proceedings of the First International Symposium*. Hemisphere, 1986; 75–86.
3. Quintiere JG. A simulation model for fire growth on materials subject to a room-corner test. *Fire Safety Journal* 1993; **20**:313–339.
4. Quintiere JG, Haynes G, Rhodes BT. Applications of a model to predict flame spread over interior finish materials in a compartment. *Journal of Fire Protection Engineering* 1995; **7**(1):1–13.
5. Mowrer FW. Dehydration of painted gypsum wallboard subjected to fire heat fluxes. In preparation.
6. Pickard RW. The fire hazard of surface coatings. *Paint Manufacture* 1954; 426–430.
7. Murrell J, Rawlins P. Fire hazard of multilayer paint surfaces. *Fire and Materials—Proceedings of the 4th International Conference and Exhibition*, 1995; 329–338.
8. McGraw JR, Mowrer FW. Flammability and dehydration of painted gypsum wallboard subjected to fire heat fluxes, to appear in *Fire Safety Science—Proceedings of the Sixth International Symposium*, 2000; 12.
9. Mowrer FW, McGraw R. Flammability of painted gypsum wallboard subjected to fire heat fluxes. *Interflam '99—Proceedings of the Eighth International Conference*, vol. 2, 1999; 1325–1330.
10. Spinn JP. USG Corporation, Personal communication.
11. Duron Corporation. Technical Data, Duron Everlast Interior Alkyd/Oil Semi-Gloss Enamel Bases, Rev. January, 1999.
12. Duron Inc. Material Safety Data Sheet, Duron Everlast Interior Alkyd/Oil Semi-Gloss Enamel Bases, Rev. June, 2000.
13. NFPA 271. *Standard Method of Test for Heat and Visible Smoke Release Rates for Materials and Products Using an Oxygen Consumption Calorimeter*. National Fire Protection Association, 1998.
14. ASTM E1354. *Standard Test Method for Heat and Visible Smoke Release Rates for Materials and Products Using an Oxygen Consumption Calorimeter*. American Society for Testing and Materials, 2000.
15. Messerschmidt B, van Hees P. Influence of delay times and response times on heat release measurements. *Fire and Materials* 2000; **24**:121–130.
16. Dillon SE, Kim WH, Quintiere JG. Determination of Properties and the Prediction of the Energy Release Rate of Materials in the ISO 9705 Room-Corner Test. *NIST GCR 98-753*, National Institute of Standards and Technology. Gaithersburg: MD; 1998.
17. Mowrer FW, Williamson RB. Flame spread evaluation for thin interior finish materials. *Fire Safety Science—Proceedings of the Third International Symposium*, Cox G, Langford B (eds). Elsevier Applied Science: New York, 1991; 689–698.
18. Tewarson A. Generation of heat and chemical compounds in fires, Chapters *3–4, SFPE Handbook of Fire Protection Engineering* (2nd edn). National Fire Protection Association, 1995; 3-53–3-124.

19. Quintiere JG. Surface flame spread, Chapters 2–14, *SFPE Handbook of Fire Protection Engineering* (2nd edn). National Fire Protection Association, 1995; 2-205–2-216.
20. ASTM E1321, *Standard Test Method for Determining Material Ignition and Flame Spread Properties*. American Society for Testing and Materials, 1997.
21. Hopkins Jr D, Quintiere JG. Material fire properties and predictions for thermoplastics. *Fire Safety Journal* 1996; **26**(3):241–268.
22. Rhodes BT, Quintiere JG. Burning rate and heat flux for PMMA in the cone calorimeter. *Fire Safety Journal* 1996; **26**(3):221–240.

